ISSN 2075-1133, Inorganic Materials: Applied Research, 2019, Vol. 10, No. 3, pp. 503–511. © Pleiades Publishing, Ltd., 2019.
Russian Text © The Author(s), 2018, published in Fizika i Khimiya Obrabotki Materialov, 2018, No. 2, pp. 19–30.

EFFECTS OF ENERGY FLUXES ON MATERIALS

Influence of Pulsed Beams of Deuterium Ions and Deuterium Plasma on the Aluminum Alloy of Al–Mg–Li System

V. N. Pimenov[a, *], G. G. Bondarenko[b, **], E. V. Dyomina[a, *], S. A. Maslyaev[a, ****], V. A. Gribkov[a, *****], I. P. Sasinovskaya[a, ******], N. A. Epifanov[a, b, *******], V. P. Sirotinkin[a, ********], G. S. Sprygin[a, *********], A. I. Gaydar[c, **********], and M. Paduch[d, ***********]**

[a] *Baikov Institute of Metallurgy and Materials Science, Russian Academy of Sciences, Moscow, 119334 Russia*
[b] *National Research University High School of Economics, Moscow, 101000 Russia*
[c] *Scientific Research Institute of Advanced Materials and Technologies, Moscow, 115054 Russia*
[d] *Institute of Plasma Physics and Laser Microfusion, Warsaw, 01-497 Poland*
**e-mail: pimval@mail.ru*
***e-mail: gbondarenko@hse.ru*
****e-mail: elenadyom@mail.ru*
*****e-mail: maslyaev@mail.ru*
******e-mail: gribkovv@rambler.ru*
*******e-mail: porfirievna@mail.ru*
********e-mail: mophix94@gmail.com*
*********e-mail: sir@imet.ac.ru*
**********e-mail: engaer@rambler.ru*
***********e-mail: niipmt@mail.ru*
************e-mail: marian.paduch@ifpilm.pl*

Received March 14, 2018; revised March 14, 2018; accepted March 14, 2018

Abstract—The damage and structural state of the surface layer of Al–Li–Mg samples composed of Al–5% Mg–2% Li (wt %) under pulsed action of power streams of high-temperature deuterium plasma and high-energy deuterium ions in the Plasma Focus (PF) device have been investigated. The radiation power density was $q \sim 10^6$ W/cm^2; the pulse duration was 50–100 ns. Pulsed thermal heating and rapid cooling is established to lead to the melting and solidification of a thin surface layer of the alloy for several tens of nanoseconds. At the same time, in the superheated surface layer of the alloy, microcavities of a spherical shape are formed which is associated with intense evaporation of lithium into micropores within the heated layer. Thermal stresses caused by abrupt heating, melting, and cooling of a thin surface layer of metal result in formation of microcracks in the near-surface zone of the samples. The evaporation by the power electron beam of the elements of the anode material of the PF device (copper and tungsten) and their subsequent deposition onto the irradiated surface of the investigated samples in the form of droplets of submicron size are noted. It is shown that the thermal and radiation-stimulated processes generated in the alloy under the action of pulsed energy fluxes in the implemented irradiation regime lead to the redistribution of elements in the surface layer of the aluminum solution, contributing to an increase in magnesium content and the formation of magnesium oxide on the surface.

Keywords: Al–Mg–Li alloy, plasma focus, dense deuterium plasma, fast deuterium ion beam, surface damage, surface modification

DOI: 10.1134/S207511331903033X

INTRODUCTION

It is known that aluminum alloys of the Al–Mg–Li, Al–Cu–Li, Al–Mg–Cu–Li, and other systems have good corrosion resistance, low density, fairly high specific strength, good processability, and very high modulus of elasticity [1–5]. For this reason, they are widely used as construction materials in the transport engineering industry, chemical industry, and aviation and space technology. A well-balanced set of mechanical properties makes these alloys particularly promising for use in the aerospace industry [6].

The binary Al–Li alloys with a low (1–3 wt %) lithium content belong to the so-called sweating alloys, since the surface in these alloys is substantially lithium-enriched owing to Gibbs thermal segregation [7].

One of the pioneers in studying the radiation and thermal properties of Al–Li alloys was L.I. Ivanov, who initiated the work in this direction [7–16]. It was shown in [8] that Gibbs segregation increases with the isothermal exposure of the Al-Li alloy at elevated (up to ~500°C) temperatures despite the loss of lithium because of its evaporation. Irradiation of the alloy at low temperatures (~50°C) with hydrogen, helium, and oxygen ions also leads to significant enrichment of the surface in lithium owing to the radiation-induced segregation, despite the continuous sputtering of a lithium-rich surface layer by an ion beam [9]. This property of the binary Al–Li alloys associated with the increase in the lithium content on the surface (the "sweating effect") due to Gibbs thermal segregation or due to radiation-stimulated processes enhances the emission properties of the material. The coefficient of secondary electron emission of this alloy is 7 [10], and for this reason, the Al–Li alloys are considered promising for the use in the electronics industry as sources of electron emission in electrovacuum devices. It is important to note that cathodes made of such alloys have, in addition to high emissivity, increased resistance to cathode sputtering and durability. In particular, it was experimentally shown in [11] that, owing to the self-healing effect of a lithium layer sputtered during irradiation with helium ions with the energy of 2.5 keV, the resistance to ion sputtering of the surface of the Al–3% Li alloy was four times higher than that of aluminum. The durability of secondary-emission cold Al–Li cathodes of helium–neon lasers bombarded with helium and neon ions in the working process exceeded 10^5 h [12], which is more than a half order of magnitude higher than that of aluminum cathodes.

The Al-Li alloys are also used as cathodes of electron-beam guns of the high-voltage glow discharge (HGD) of smelting metallurgical plants, which provide an electron beam of several hundred kilowatts. Testing of an HGD gun with a cathode with the diameter of 100 mm from Al–2% Li alloy showed [13] a long-term continuous stable operation of the cathode during industrial smelting with the fluence of bombarding hydrogen particles (working gas) of more than 10^{22} cm^{-2} and the heat flux density of ~0.5–1.0 kW/cm^2. A characteristic feature of this kind of experiments performed on alloys of the Al–Li, Al–Mg–Li, Al–Cu–Li, and Al–Cu–Mg–Li systems [13–15] is the proximity of the irradiation conditions (the thermal load of 15 MW/m^2, particle flux density of 10^{17}–10^{18} cm^{-2} s^{-1}, fluence of 10^{20}–10^{22} cm^{-2}) to the real conditions of radiation effects on the materials of the first wall and divertor plates of a fusion reactor with magnetic confinement of the plasma.

Adding Al–(1.8–2.3) wt % Li to the alloy in the amount of 4.5–6.0 wt % hardly affects the character of the Li segregation to the surface during irradiation with helium ions with the energy of $E = 75$ keV to the dose of ~10^{16}–10^{17} ion/cm^2 [16]. However the Mg concentration on the irradiated surface decreases in comparison with its content in the bulk, which is explained by the higher binding energy of the "dissolved Li atom–vacancy" complex (0.23 eV) in comparison with the "dissolved Mg atom–vacancy" complex (0.04 eV) in aluminum [17] and, as a result, the more intense radiation-stimulated lithium segregation on such a powerful sink as the surface.

The ion-beam treatment of the Al–Li alloys is of increased interest from the point of view of modifying and improving their physicomechanical properties owing to the influence of radiation-dynamic effects. In particular, the effect of beams of accelerated Ar^+ ions with the energy of 40 keV on the samples of the cold-deformed alloy 1441 of the Al–Cu–Mg–Li system in the form of stripes initiates the course of the process of radiation annealing (RA), which is many times faster than thermal annealing [18, 19]. In this case, the RA proceeds at lower temperatures throughout the entire volume of the band with a thickness of 1–3 mm despite the significantly smaller (by several orders of magnitude) average projective path of the Ar^+ ions with the energy of 40 keV in aluminum alloys (~40 nm). The recrystallization processes implemented in the 1441 alloy during the RA, accompanied by the grain growth and the change in the structural phase state as a result of the dissolution of intermetallic compounds of the crystallization origin and the formation of new phases, ensure the formation of mechanical properties combining high strength with significantly increased plasticity of the alloy [20].

The studies on the effects of pulsed laser radiation (LR) in the free generation mode on samples of the aluminum alloy 1420 of the Al–Mg–Li system [21] revealed an unusual character of the damage to the irradiated surface layer associated with its melting and the formation of a set of spherical pores in it in the process of the high-temperature heating and cooling. Such intense pore formation in the surface layer was not observed at the high-power pulse impacts of ions, plasma, and LR either in pure aluminum or in alloys and compositions based on it that do not contain lithium [22–26]. It is natural to assume that the intense evaporation of lithium, which is part of the alloy 1420, accompanied by the formation of bubbles in the liquid phase, leads to the formation of the high concentration of pores in the hardened surface layer.

This work is a continuation of the cycle of research conducted under the guidance of L.I. Ivanov by his colleagues and students [7–16] and is devoted to the study of the damage and the structural state of the surface layer of the aluminum alloy 1420 of the Al–Mg–Li system with the simultaneous complex effect of the fluxes of the high-energy deuterium ions and high-temperature deuterium plasma in the Plasma Focus (PF) facility. In this case, the irradiation regime was close to the conditions of the radiation load on the material facing the plasma in the working chamber of a fusion plant with inertial plasma confinement.

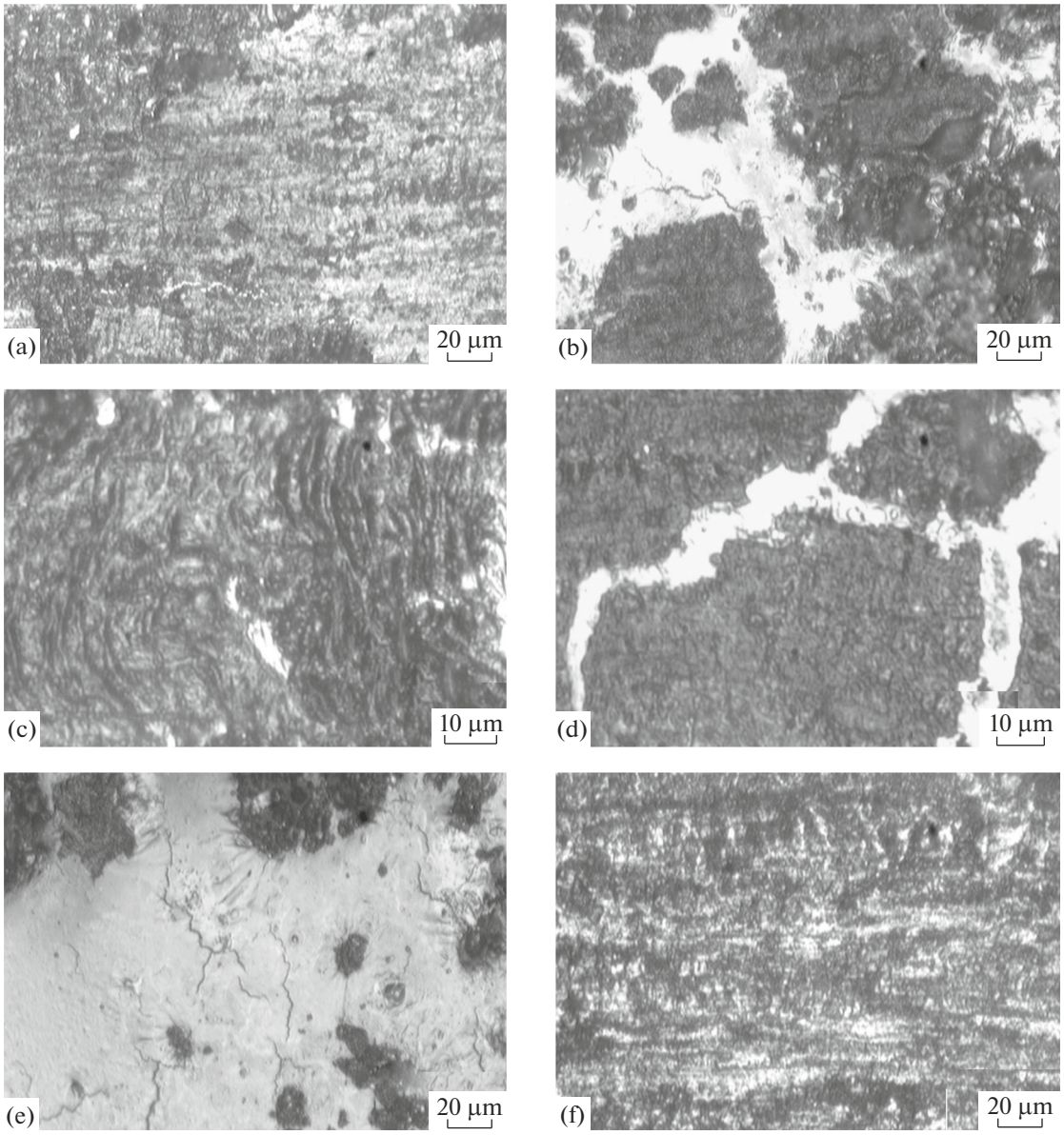

Fig. 1. Optical images of different sections of the initial surface (f) and the surface irradiated with deuterium plasma and deuterium ions: (a) surface without damage to the oxide film; (b, d) surface areas with different degrees of damage to the oxide film; (c) wavy relief of the molten surface; (e) microcracks on the area of the alloy surface that is free of oxide film after irradiation.

MATERIALS AND METHODS

The aluminum alloy 1420 contained 2 wt % Li and 5 wt % Mg. The samples for irradiation were plates with a thickness of 2 mm and a size of 25 × 25 mm. The treatment with ion and plasma fluxes was carried out on a PF-1000 device (Warsaw, Poland). When irradiated, the samples were located in the cathode part of the discharge chamber at a distance of 40 cm from the anode of the device . Deuterium was used as the working gas at a pressure of $P \approx 1–2$ Pa. The power density of the ion and plasma fluxes was 5×10^6 W/cm^2 at the ion pulse duration $t_i = 50$ ns and the plasma flux duration $t_p = 100$ ns. The number of pulse impacts on each sample was $N = 4$.

After irradiation, the samples were examined by metallography methods on a NEOPHOT-32 optical microscope using a scanning electron microscope with an EVO 40 X-ray spectral analyzer (Zeiss) and also by the atomic emission analysis on a GDS-850A glow discharge spectrometer.

The phase composition of the surface layer was analyzed by X-ray diffractometry on a Rugaky (XRD) Ultima-IV diffractometer (Japan). The temperature distribution in the surface layer in the direction perpendicular to the irradiated surface was calculated on the basis of a one-dimensional model similar to that described in [27].

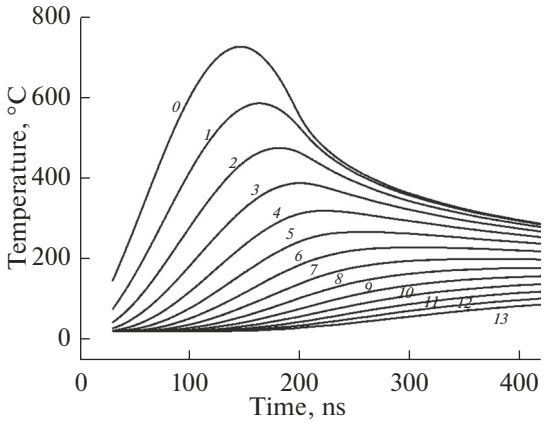

Fig. 2. Evolution of temperature with time from the onset of the action of the pulse at various distances from the irradiated surface of the alloy sample (the distances are denoted by numbers from 0 to 13 μm).

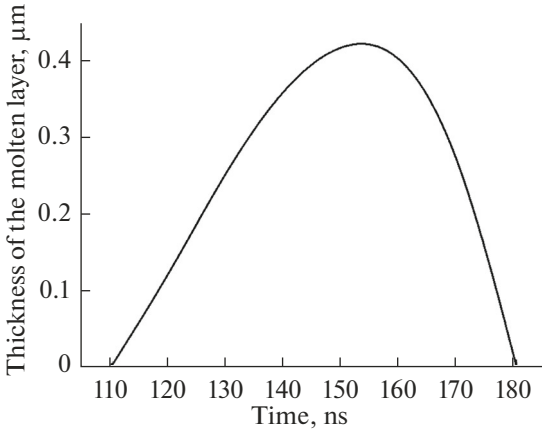

Fig. 3. Time variation of the thickness of the molten layer on the surface of the irradiated alloy sample.

RESULTS AND DISCUSSION

Optical Microscopy

The degree of radiation-thermal erosion of the material was estimated by the change in the mass of the material during irradiation. The results of weighing samples before and after pulsed irradiation showed that, in the implemented irradiation modes, their mass does not change within the limits of the measurement accuracy (±0.05 mg), which indicates the approximate balance of the mass of evaporated and precipitated substances. Figure 1 shows photomicrographs of the surface of the samples before (Fig. 1f) and after exposure to four pulses in the PF-1000 device at the average energy flux density of 5×10^6 W/cm^2 (Figs. 1a–1e).

The study of the irradiated surface showed that a significant part of it had no visible signs of damage (Fig. 1a) and did not significantly differ from the original surface (Fig. 1f). In some regions of the surface layer, traces of melting are observed. It should be noted that the significant part of the surface is covered with a thin oxide film, which after irradiation remains unmelted. At the same time, the surface layer beneath this film is melted to form a wavy relief in some regions of the crystallized alloy (Fig. 1c). At the same time, a thin, more refractory, film remaining in the solid state mimics the topography of the deformed surface relief formed during the process of thermal heating and cooling of the surface layer (Fig. 1c). It can be assumed that this film contains refractory oxides of the alloy elements that do not melt in the irradiation regime implemented in our experiments. In the regions of the irradiated surface where the oxide film is damaged (Figs. 1b, 1d, 1e), microcracks are visible on the film-free metal surface (Fig. 1e), which are formed under the action of thermal stresses during the alloy solidification.

Numerical Calculation of the Temperature Distribution in the Surface Layer

The numerical analysis of the thermal effect of irradiation on the material was carried out for a pulsed energy flux with the power density of $q = 5 \times 10^6$ W/cm^2 and the total pulse time $t = 200$ ns. The calculation results for different distances x into depth from the surface are shown in Fig. 2. It can be seen that the temperature directly on the surface ($x = 0$) exceeded the melting point of the material (~660°C), which led to its melting and the formation of a wavelike surface relief with a refractory film located on it. The formation of a wavy relief is due to the pressure from the plasma and the reactive effect of the vapor flow from a thin surface layer of the molten metal.

In this case, as already noted, melting did not occur over the entire irradiation area, but in separate local regions of the surface. This fact indicates the nonuniformity in the distribution of the energy flux density in the beam of particles (ions and plasma) incident on the sample. At the displacement from the surface into the depth of the material of $x \geq 1$ μm, the estimates show that the alloy temperature did not reach its melting threshold and the surface layer in this zone remained in the solid state.

Figure 3 shows the change in the calculated layer thickness of the liquid phase during irradiation. It can be seen that the lifetime of the liquid phase was ~70 ns, and the maximum thickness of the molten layer was $h_{max} \approx 0.4$ μm.

Scanning Electron Microscopy and X-ray Analysis

The X-ray spectrum from the surface of the initial sample (Fig. 4) shows the lines of the main alloy elements, aluminum and magnesium (with the exception of lithium, which is not fixed by this method). The oxygen line is also present, indicating its presence in the composition of the oxide film on the surface of the initial samples.

The scanning electron microscopy analysis of the irradiated samples showed that dark spots of various

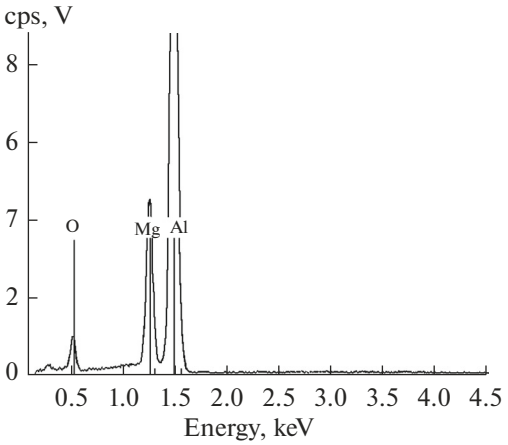

Fig. 4. Elemental composition of the surface of the original Al–Li–Mg alloy from X-ray spectral analysis.

sizes from fractions of a micron to about two microns are visible in the form of regular circles with diffuse edges on the surface regions free from the oxide film (Figs. 5a, 5d). It can be assumed that these are projections of spherical cavities located near the irradiated surface, which were formed in the zone of elevated temperature with the intense internal evaporation of lithium dissolved in aluminum. The characteristic dimensions of the cavities are comparable with the maximum layer thickness of the liquid phase formed on the surface of the samples during the impact of the energy pulse on the alloy under study. There are also a significant number of larger cavities. Apparently, there was evaporation of lithium into internal micropores, which occurred in both the solid and liquid phases under heating of the surface layer of the alloy to several hundred degrees (Fig. 2). Previously, the formation of such pores in the near-surface region of the alloy under study was observed under laser irradiation of the alloy in the free generation mode [21].

Electron microscopic analysis with a sufficiently large magnification (×25000) showed that the surface regions on which the original oxide film was preserved were covered with metal droplets having the size from tens to hundreds of nanometers, which were deposited after the material was evaporated by an electron beam from the surface of the anode of the PF installation (droplets are visible in Fig. 5c as light points). The X-ray analysis of the composition of surface regions with droplets deposited on them showed a high copper and tungsten content in these areas, i.e., those elements that are the main components of the composition of the material of the anode unit of the working chamber of the PF-1000 facility.

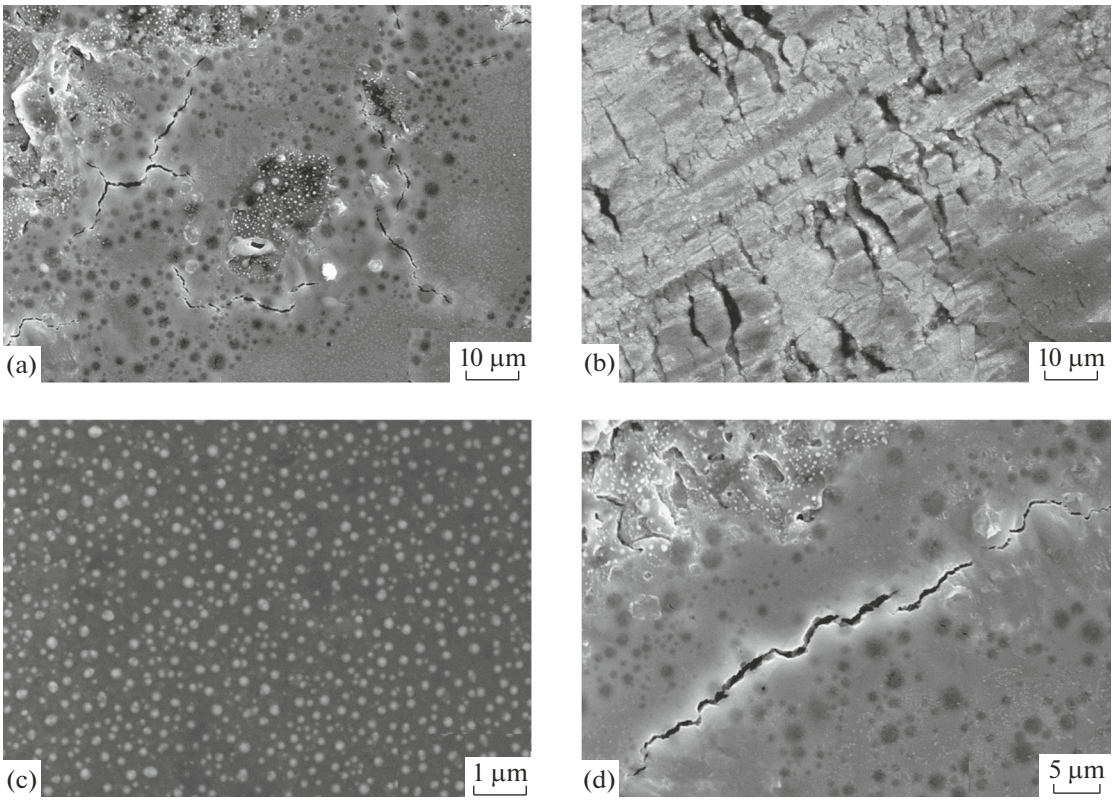

Fig. 5. SEM images of the initial surface (b) of the alloy 1420 and various surface regions after irradiation in the PF-1000 device: (a) general view of the irradiated surface with areas covered with oxide film and areas free of oxide film; (c) the surface area of the oxide film with droplets of precipitated metal (light points); (d) microcrack on the sample surface area free of oxide film and pores under the surface (dark spots of rounded shape).

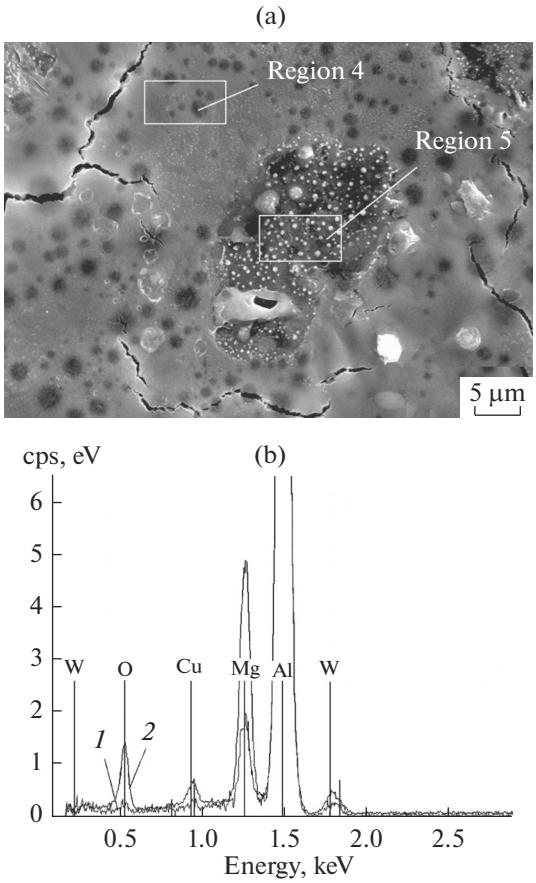

Fig. 6. SEM image of irradiated surface (a) and elemental composition (b) of the region of the surface with the oxide film (region 5, curve *1*) and the area of irradiated surface free of the oxide film (region 4, curve *2*).

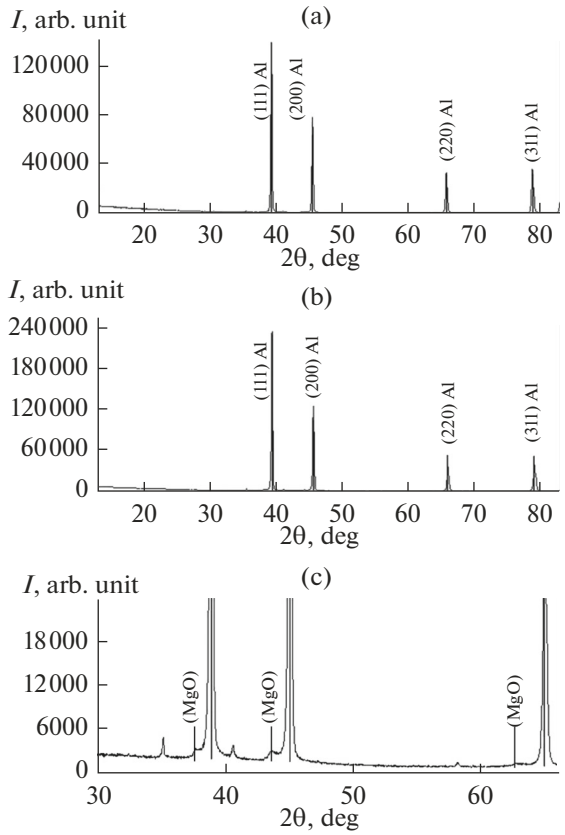

Fig. 7. X-ray diffraction pattern of the alloy 1420 in the initial state (a) and after irradiation (b). Peaks of MgO phase are shown on an enlarged scale (c).

For comparison, Fig. 6 shows the X-ray spectra taken from two sections of the surface of the irradiated sample—covered with the oxide film (region 5) and free from this film (region 4). It can be seen that the elemental composition of the surface in region 5 (curve *2*) is qualitatively close to the composition of the initial sample coated with the oxide film, and the spectrum in region 5 shows bursts of lines corresponding to aluminum, magnesium, oxygen, and also elements deposited from the anode part of the chamber (Cu, W). The absence of the deposited Cu and W droplets in the regions free from the oxide film is due to the fact that gaps in the film were formed after the end of the plasma pulse effect on the target sample and the associated vaporized flow and microdroplets from the surface of the anode material of the PF chamber. There is a slight increase in the magnesium content in the zone where the oxide film is located (curve *2*, region 5) as compared with the region free of the film (curve *1*, region 4). This fact indicates the redistribution of this element, related to the fact that a part of magnesium in the Al-based solid solution is spent on the formation of the oxide film. Therefore, in the zone adjacent to it, the surface layer of the alloy is depleted in magnesium. Owing to the sharp increase in temperature by several hundred degrees under the pulse impact of the energy flux on the alloy (Fig. 2) and intense evaporation of lithium from the surface layer of the alloy through the irradiated surface and into micropores (Figs. 5a, 5d, 6), its amount in the Al-based solid solution decreases and, accordingly, the Mg content increases. In this case, an increased nonequilibrium concentration of vacancies is also generated.

These results show that, in the irradiation regime used in our experiments, the combined effect of thermally and radiation-stimulated processes contributes to a certain depletion of the surface layer of the aluminum alloy in lithium owing to its evaporation into the pores and the diffusion exit to the surface and enrichment in magnesium. To a greater extent, this result corresponds to the surface regions covered with the oxide film, which impedes sputtering and evaporation processes.

X-ray Phase Analysis

The phase composition of the samples before and after irradiation was studied by X-ray diffraction analysis. In the diffraction pattern of the alloy in the initial state, the lines corresponding to the crystal lattice of the solid solution of magnesium in aluminum and very weak traces of lines of magnesium oxide MgO (Fig. 7a)

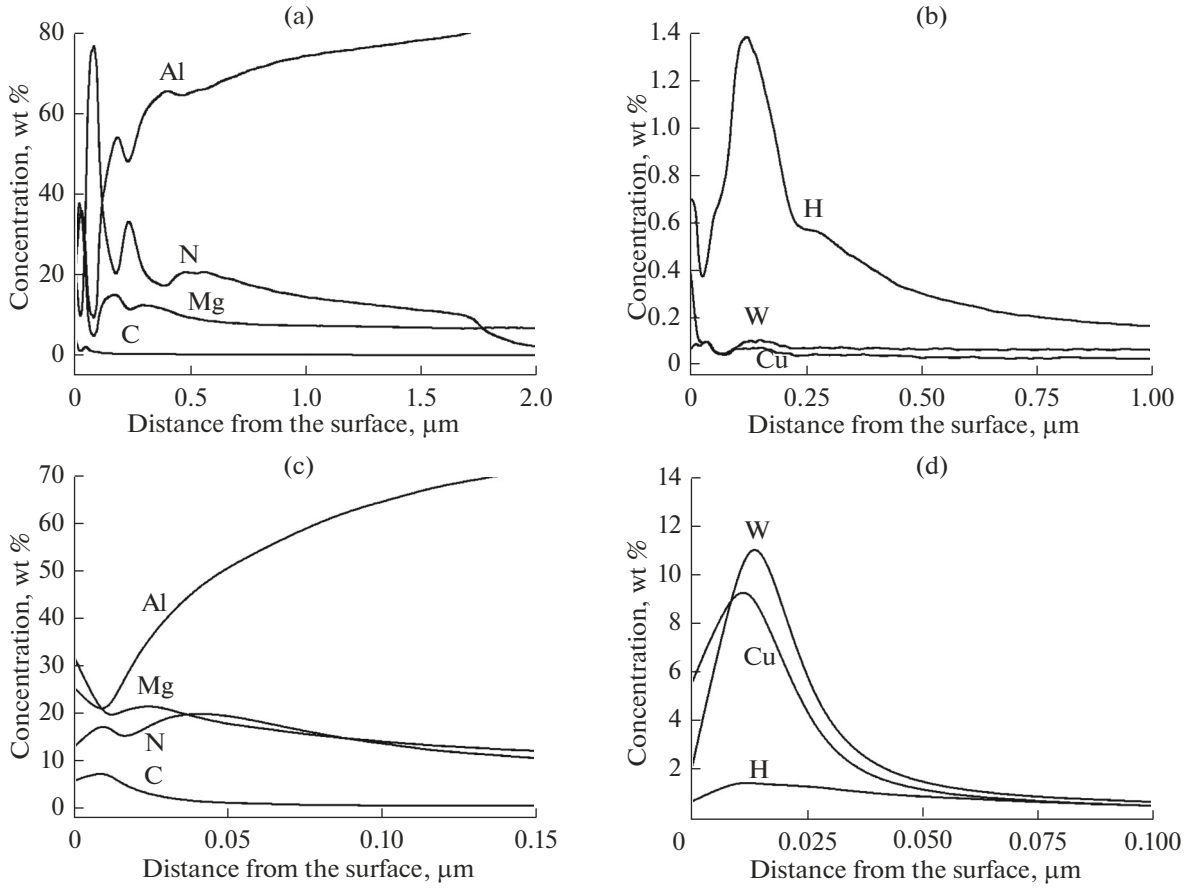

Fig. 8. Distribution of elements in the surface layer of the sample of the studied alloy in the initial state (a, b) and after irradiation (c, d) from the atomic emission spectroscopy data: (a, c) Al, N, Mg, C; (b, d) W, Cu, H.

are visible. After irradiation, the phase composition of the samples does not change qualitatively (Figs. 7b, 7c), and the crystal lattice of the aluminum-based solid solution is fixed in the surface layer, as in the starting material. However, the lattice parameter of this solid solution decreases markedly as a result of the exposure to ion and plasma fluxes: before irradiation, a = 4.0720 Å, and after irradiation, a = 4.0652 Å, which indicates certain structural changes occurring in Al solid solution in the temperature gradient field and the redistribution of elements in the surface layer.

The lines corresponding to the amount of magnesium oxide that slightly increased compared with the initial state are shown in the diffraction pattern recorded on an enlarged scale (Fig. 7c). Microgroplets of deposited metals observed during the electron microscopic examination do not give traces on the diffraction patterns of the samples after irradiation, which is apparently associated with the small amount of deposited material and, possibly, with the amorphous droplet structure, which hardened at the high cooling rate of ~10^7 K/s.

Atomic Emission Spectral Analysis

Figure 8 shows the distribution curves of elements in the surface layer of the alloy in the initial state and after irradiation recorded by atomic emission spectroscopy (AES). In general, the AES results are consistent with the X-ray analysis data and confirm the presence of deposited W and Cu droplets on the irradiated surface. However, there is nitrogen in the surface layer of the original alloy with the thickness of ~2 μm, which, apparently, got into the material at the stage of preparation of the alloy. After irradiation, its content in the thin layer ~150 nm thick decreases. It is significant that a noticeable increase in the Mg concentration is observed in this very thin layer after irradiation from 5–7% before irradiation to ~15% at the depth of 150 nm and to 20 wt % directly on the surface after the plasma beam effect. This effect of the increase in the Mg concentration on the surface is opposite to the effect of the decrease in the Mg content in this region when the alloy of the Al–Mg–Li system is irradiated with helium ions (E = 75 keV, ~10^{16}–10^{17} ions/cm^2) [16]. This difference in the results is determined by different conditions of the experiments. In our case, the increased magnesium

concentration in the surface layer is determined by the presence of a film based on magnesium oxide, whose content slightly increases after irradiation.

CONCLUSIONS

The damageability of the surface layer of the aluminum alloy 1420 of the Al–Mg–Li system under pulsed exposure to high-power fluxes of high-temperature deuterium plasma and high-energy deuterium ions in the Plasma Focus device was studied at the radiation power density of $q = 5 \times 10^6$ W/cm^2 and the pulse duration of 50–100 ns. It was established that pulsed thermal heating and rapid cooling lead to melting and solidification of a thin surface layer of alloy samples for several tens of nanoseconds. In this case, spherical microcavities are formed in the superheated surface layer, which is associated with the intense evaporation of lithium into the micropores inside the heated layer. Thermal stresses due to rapid heating, melting, and cooling of the thin surface layer of the metal lead to the formation of microcracks in the near-surface zone of the samples. The electron beam evaporates the elements that compose the anode material of the PF device (copper and tungsten), and their subsequent deposition on the irradiated surface of the alloy samples under study in the form of droplets of submicron size is observed.

These changes in the structural-phase state of the irradiated surface layer of the alloy are associated with the increase in the magnesium oxide content in it and the decrease in the lattice parameter of the aluminum-based solid solution, probably due to the partial removal of impurity nitrogen from the irradiated surface layer.

It is shown that thermal and radiation-stimulated processes generated in the alloy under the action of pulsed energy fluxes in the implemented irradiation regime lead to the redistribution of elements in the surface layer of the studied alloy, favoring the increase in the magnesium content and the formation of the magnesium oxide film on the irradiated surface.

FUNDING

The work was performed according to the state task no. 075-00746-19-00 and was supported by the International Atomic Energy Agency, grant IAEA CRP no. 19248.

CONFLICT OF INTERESTS

The authors declare that they have no conflict of interest.

REFERENCES

1. Fridlyander, I.N., Chuistov, K.V., Berezina, A.L., and Kolobnev, N.I., *Alyuminii-litievye splavy: struktura i svoistva* (Aluminum-Lithium Alloys: Structure and Properties), Kiev: Naukova Dumka, 1992.
2. Fridlyander, I.N., Shamrai, V.F., Babareko, A.A., Kolobnev, N.I., Khokhlatov,a L.B., and Egiz, I.V., Texture of a sheet of alloy 1430 of the Al–Li–Mg–Cu system and anisotropy of its yield point, *Metally*, 1999, no. 2, pp. 79–84.
3. Rioja, R.J., Fabrication methods to manufacture isotropic Al–Li alloys and products for space and aerospace applications, *Mater. Sci. Eng., A*, 1998, vol. 257, pp. 100–107.
4. Deschamps, A., Sigli, C., Mourey, T., de Geuser, F., Lefebvre, W., and Davo, B., Experimental and modeling assessment of precipitation kinetics in an Al–Li–Mg alloy, *Acta Mater.*, 2012, vol. 60, no. 5, pp. 1917–1928.
5. Betsofen, S.Ya., Antipov, V.V., and Knyazev, M.I., Al–Cu–Li and Al–Mg–Li alloys: Phase composition, texture, and anisotropy of mechanical properties (review), *Russ. Metall.* (Moscow), 2016, vol. 2016, no. 4, pp. 326–341.
6. Betsofen, S.Ya., Antipov, V.V., Knyazev, M.I., and Oglodkov, M.S., Effect of heat treatment on the phase composition, the texture, and the mechanical properties of a V1461 (Al–Cu–Li) alloy, *Russ. Metall.* (Moscow), 2015, vol. 2015, no. 11, pp. 929–936.
7. Bondarenko, G.G. and Kucheryavyi, S.I., Surface segregation of lithium in aluminum-lithium alloys, *Fiz. Khim. Obrab. Mater.*, 1991, no. 1, pp. 132–135.
8. Bondarenko, G.G., Ivanov, L.I., and Kucheryavyi, S.I., Volatility of aluminum–lithium alloys, *Fiz. Khim. Obrab. Mater.*, 1987, no. 4, pp. 93–95.
9. Bondarenko, G.G., Ivanov, L.I., and Kucheryavyi, S.I., Segregation of lithium in Al–2.2% Li alloy, *Fiz. Khim. Obrab. Mater.*, 1985, no. 3, pp. 53–55.
10. Bondarenko, G.G. and Shishkov, A.V., Emission properties of an aluminum-lithium alloy, *J. Surf. Invest.: X-ray, Synchrotron Neutron Tech.*, 1995, vol. 11, no. 9, pp. 944–948.
11. Bondarenko, G.G., Ivanov, L.I., and Kucheryavyi, S.I., Examination of Sputtering of aluminum alloys under ion bombardment, *Fiz. Khim. Obrab. Mater.*, 1986, no. 5, pp. 24–25.
12. Bondarenko, G.G., Korzhavyi, A.P., Kristya, V.I., and Sigov, D.N., Effect of surface relief on ion sputtering of cathode materials of gas discharge lasers, *Metally*, 1993, no. 3, pp. 97–100.
13. Bondarenko, G.G., Zhirnov, O.N., Ivanov, L.I., Kucheryavyi, S.I., and Udris, Ya.Ya., Effect of hydrogen plasma on aluminum-lithium alloys, *Fiz. Khim. Obrab. Mater.*, 1992, no. 2, pp. 5–8.
14. Bondarenko, G.G. and Udris, Ya.Ya., Influence of high heat flux loading and irradiation on some promising candidate materials for the divertor structure, *Fusion Eng. Des.*, 1998, vols. 39–40, pp. 419–426.
15. Bondarenko, G.G. and Udris, Ya.Ya., Erosion of materials bombarded by intense polyenergetic beams of hydrogen particles, *Poverkhn.: Rentgenovskie, Sinkhrotronnye Neitr. Issled.*, 1999, no. 4, pp. 70–77.
16. Bondarenko, G.G., Radiation-induced processes in the near-surface layers of metal alloys, *Metally*, 1993, no. 1, pp. 150–161.

17. Ceresara, S., Giarda, A, and Sanchéz, A., Annealing of vacancies and ageing in Al–Li alloys, *Philos. Mag.*, 1977, vol. 35, no. 1, pp. 97–110.

18. Ovchinnikov, V.V., Gushchina, N.V., Makhin'ko, F.F., Chemerinskaya, L.S., Shkol'nikov, A.R., Mozharovskii, S.M., Filippov, A.V., and Kaigorodova, L.I., Structural features of aluminum alloy 1441 irradiated by Ar^+ ions, *Russ. Phys. J.*, 2007, vol. 50, no. 2, pp. 177–185.

19. Ovchinnikov, V.V., Gushchina, N.V., Mozharovsky, S.M., Filippov, A.V., Sagaradze, V.V., and Vildanova, N.F., Examination of structure of aluminum alloys AMg6 and 1441 after ion-beam treatment, *Proc. 10th Int. Conf. on Modification of Materials with Particle Beams and Plasma Flows, September 19–24, 2010, Tomsk*, Tomsk: Tomsk. Gos. Univ., 2010, pp. 305–308.

20. Ovchinnikov, V.V., Gavrilov, N.V., Gushchina, N.V., Kamenetskikh, A.S., Emlin, D.R., Mozharovskii, S.M., Filippov, A.V., and Kaigorodova, L.I., Radiation annealing of AMg6, 1441, and VD1 aluminum alloy strips using a ribbon source of accelerated ions, *Russ. Metall.* (Moscow), 2010, vol. 2010, no. 3, pp. 207–213.

21. Maslyaev, S.A., Neverov, V.I., Pimenov, V.N., and Sasinovskaya, I.P., Effect of pulse laser radiation on deformable aluminum alloys, *Fiz. Khim. Obrab. Mater.,* 1992, no. 3, pp. 34–37.

22. Pimenov, V.N., Maslyaev, S.A., Ivanov, L.I., Panin, O.V., Dyomina, E.V., Gribkov, V.A., Dubrovsky, A.V., Ugaste, Yu.E., Scholz, M., Miklaszewski, R., and Grunwald, Ya., Interaction of pulsed streams of deuterium plasma with aluminum alloy in a plasma focus device. I. A new methodology of the experiment, *Proc. Tallinn Univ. Soc. Educ. Sci., Part B*, 2003, vol. 2, pp. 30–39.

23. Pimenov, V.N., Maslyaev, S.A., Dyomina, E.V., Ivanov, L.I., Kovtun, A.V., Gribkov, V.A., Dubrovskii, A.V., and Ugaste, Yu.E., Impact of pulse energy flows on the pipe surface from aluminum alloy in the Plasma focus installation, *Perspekt. Mater.*, 2006, no. 4, pp. 43–52.

24. Pimenov, V.N., Demina, E.V., Maslyaev, S.A., Ivanov, L.I., Gribkov, V.A., Dubrovskii, A.V., Ugaste, Ü.E., Laas, T., Scholz, M., Miklaszewski, R., Kolman, B., and Tartari, A., Damage and modification of materials produced by pulsed ion and plasma streams in dense Plasma Focus device, *Nukleonika*, 2008, vol. 53, no. 3, pp. 111–121.

25. Maslyaev, S.A., Morozov, E.V., Romakhin, P.A., Pimenov, V.N., Gribkov, V.A., Tikhonov, A.N., Bondarenko, G.G., Dubrovsky, A.V., Kazilin, E.E., Sasinovskaya, I.P., and Sinitsyna, O.V., Damage of Al_2O_3 ceramics under the action of pulsed ion and plasma fluxes and laser irradiation, *Inorg. Mater.: Appl. Res.*, 2016, vol. 7, no. 3, pp. 330–339.

26. Epifanov, N.A., Bondarenko, G.G., Demin, A.S., Morozov, E.V., Gribkov, V.A., Pimenov, V.N., and Maslyaev, S.A., Effect of pulse laser radiation, deuterium ion fluxes, and a dense plasma on the surface of aluminum samples with a ceramic coating based on Al_2O_3, *Trudy XXVII mezhdunarodnoi konferentsii "Radiatsionnaya fizika tverdogo tela," Sevastopol', 10–15 iyulya 2017*, (Proc. XXVII Int. Conf. "Radiation Physics of the Solids," Sevastopol, July 10–15, 2017), Moscow: Nauchno-Issled. Inst. Perspekt. Mater. Tekhnol., 2017, pp. 59–63.

27. Maslyaev, S.A., Thermal effects under pulsed irradiation of materials in the Plasma Focus device, *Perspekt. Mater.,* 2007, no. 5, pp. 47–55.

28. Bondarenko, G.G., *Radiatsionnaya fizika, struktura i prochnost' tverdykh tel* (Radiation Physics, Structure, and Strength of Solids), Moscow: Laboratoriya Znanii, 2016.

Translated by L. Mosina